Appl. Magn. Reson. 16, 481–492 (1999)

Applied Magnetic Resonance

A Model of Spin Catalysis in Bacterial Photosynthetic Reaction Centres

A. I. Ivanov, V. A. Mikhailova, and S. V. Feskov

Department of Physics, Volgograd State University, Volgograd, Russian Federation

Received October 14, 1998; revised February 2, 1999

Abstract. A model of influence of non-heme Fe^{2+} ion on kinetics of electron transfer between quinone anion-radicals Q_A^- and Q_B^- in bacterial reaction centres is proposed and investigated. Physical mechanism of the influence is associated with singlet-triplet transitions in $Q_A^-Q_B^-$ pair caused by interactions with paramagnetic Fe^{2+}. The model incorporates exchange couplings between the particles and zero-field splittings in high-spin Fe^{2+}. These interactions are shown to catalyze electron transfer in triplet pairs and alter the reaction yield significantly.

1 Introduction

Chemical reactions with participation of paramagnetic particles are known to be sensitive to certain kinds of magnetic and spin interactions experienced by reactants. A distinctive feature of these interactions is their ability to induce electron spin conversion in a reacting pair and in this way affect the dynamics of spin-selective process [1]. The influence of these interactions on product yield in many cases may be significant and amounts to tens of per cent.

One of the interesting examples of spin effects in chemical reactions is a phenomenon of spin catalysis in radical recombination (see, for example, [2, 3]). Physical mechanism of the phenomenon is based on singlet-triplet (ST) transitions in radical pair (RP) caused by exchange interactions with a third paramagnetic particle. ST-conversion of RP removes spin forbiddance for triplet recombination and results in an alteration of reaction kinetics and product yield [2–5].

In this paper a model of spin catalysis in a quinone acceptor complex Q_AQ_B of bacterial photosynthetic reaction centre (RC) is investigated. It is well known

* Presented at the Joint 29th AMPERE and 13th ISMAR International Conference on Magnetic Resonance and Related Phenomena, Berlin, August 2–7, 1998.

[6, 7] that the electron transfer (ET) reaction in the quinone complex is a two-stage ET process involving the intermediate anion-radical state of quinone pair $Q_A^- Q_B^-$. ET from the primary quinone Q_A to the secondary quinone Q_B occurs in the presence of a nearby Fe ion [6–11]. Steady-state Mössbauer experiments [11, 12] on unreduced RCs have shown that the oxidation state of Fe is +2 with a high-spin electronic ground state ($S = 2$). It is also known [13] that the valency of the Fe-ion is not changed during the ET reaction. The functional role of Fe is unclear. It has been postulated that it may be involved in: (a) determining the redox potentials and proton binding of the quinone/semiquinone couple; (b) facilitating ET between the quinones by direct orbital overlap; (c) and others (reviewed in [14, 15]). In this paper we suggest that the Fe^{2+} in bacterial RC can act as a spin catalyst facilitating ET in triplet $^3(Q_A^- Q_B^-)$ pairs through initiating the singlet-triplet mixing.

It has been found experimentally that the primary stages of the charge separation in RC

$$P^* I Q_A \rightarrow P^+ I^- Q_A \rightarrow P^+ I Q_A^- \tag{1}$$

are not sensitive to interactions with Fe^{2+} [16, 17]. Reconstitution of the Fe-depleted RC with diamagnetic Zn^{2+} essentially restores the native ET kinetics, so the dominant role of the Fe^{2+} on these stages (Eq. (1)) is not associated with its spin or magnetic interactions [16].

It is reasonable to suppose that the ET reaction in anion-radical $Q_A^- Q_B^-$ pair becomes more sensitive to magnetic interactions. Low-temperature EPR [13], magnetic susceptibility [18] and Mössbauer studies on bacterial reaction centres [11, 12] have established weak exchange couplings between Fe and quinone anion-radicals (of order of 0.5 cm^{-1}). Experimental data appearing in Fe^{2+} in [19] are indicative of an anisotropy of these interactions. However, referring to [20], the expected magnitude of maximum of anisotropic exchange coupling is approximately to $0.02J$, where J is a parameter of isotropic exchange interaction. Hereafter we restrict our consideration to the isotropic spin coupling. These interactions are likely to give the most efficient mechanism for singlet-triplet mixing in $Q_A^- Q_B^-$ since spin-spin couplings in Fe-quinone complex far exceed other spin interactions (hyperfine, dipole-dipole). For example, electron dipole-dipole coupling [20] is expected to be at least an order of magnitude smaller than the isotropic exchange interactions.

The analysis of EPR spectra [18–20] of the reduced quinone-iron acceptor complex from bacterial RC allows one to assume that the $Fe^{2+}Q_B^{2-}$ is not paramagnetic. This fact suggests that the efficiency of direct ET in triplet pairs should be low in comparison with the ET in singlet pairs. Hereafter we admit that the electron transfer takes place predominantly in singlet pairs.

In this paper we present quantum mechanical calculation of dynamics of ET between quinone anion-radicals

$$Q_A^- Fe^{2+} Q_B^- \rightarrow Q_A Fe^{2+} Q_B^{2-} \ . \tag{2}$$

The model accounts for isotropic spin exchange between the particles and zero-field splittings (ZFS) in high-spin Fe^{2+}. The aim of the study is elucidation of a possible influence of the Fe-ion on the reaction yield Eq. (2) through the spin-catalytic mechanism. Effects of exchange couplings and ZFS on the efficiency of the ET are discussed. Chemically induced electron spin polarization (CIDEP) of Fe^{2+} is investigated.

2 Model

We will follow the standard approach [1, 21–23], and take as a starting point the well-known Liouville equation

$$\frac{\partial \rho}{\partial t} = -i[\mathscr{H}, \rho] - \frac{k_S}{2}(\mathbf{P}_S \rho + \rho \mathbf{P}_S) - k\rho \quad , \tag{3}$$

where ρ is the spin density matrix, $\mathscr{H}$ is spin Hamiltonian of the complex. The second term in Eq. (3) describes the direct ET in singlet pairs $^1(Q_A^- Q_B^-)$ with the rate constant k_S, $\mathbf{P}_S$ is a projection operator on the singlet state. The last term represents spin-independent kinetic decay of reactants due to back electron recombination of Q_A^- with the primary electron donor P^+.

Spin Hamiltonian of the system is given by

$$\mathscr{H} = \mathscr{H}_{ex} + \mathscr{H}_{Fe} \ . \tag{4a}$$

Here $\mathscr{H}_{ex}$ is the Hamiltonian of spin couplings

$$\mathscr{H}_{ex} = J_0\left(\frac{1}{2} + 2\mathbf{S}_1 \cdot \mathbf{S}_2\right) + \sum_{i=1}^{2} J_i\left(\frac{1}{2} + 2\mathbf{S}_i \cdot \mathbf{S}_3\right) \ , \tag{4b}$$

J_0 is a parameter of exchange interaction between unpaired electrons of Q_A^- and Q_B^-, J_1 (J_2) – between Fe^{2+} and Q_A^- (Q_B^-).

ZFS in the high-spin Fe^{2+} ion are described by the spin Hamiltonian [18]

$$\mathscr{H}_{Fe} = DS_{3Z}^2 + E(S_{3X}^2 - S_{3Y}^2) \ , \tag{4c}$$

with D and E being the axial and orthorhombic ZFS parameters. For Fe^{2+} from *Rhodobacter sphaeroides* they are [18]: $D = 5.28$ cm^{-1}, $E = 1.33$ cm^{-1}.

Before proceeding to consideration of reaction dynamics we should make the following remark. Spin dynamics of systems containing paramagnetic (especially high-spin) particles in some cases can be significantly influenced by paramagnetic relaxation. It is known that the relaxation tends to randomize orientations of spins of particles and often provides additional mechanisms for spin conversion in reactants. In this paper we admit a simplified model for

spin dynamics which does not take into account relaxation effects. Note that the rate of singlet-triplet transitions in the three-spin model is determined by the parameter $|J_1 - J_2|$. Thus, the limit of validity of this model can be roughly estimated by $|J_1 - J_2|T \gg 1$, where T is a paramagnetic relaxation time.

Basis spin functions of Fe-quinone complex are taken as a composition of eigenstates of Hamiltonian Eq. (4a), when $J_1 = J_2 = 0$

$$\Psi^{(i)} = \Psi^{\kappa}_{\mathrm{Fe}} \Psi^{j}_{\mathrm{Q}} \ , \qquad i = 1, ..., 20 \ . \tag{5}$$

Here $\Psi^{\kappa}_{\mathrm{Fe}}$ ($k = 1, ..., 5$) denote the spin wavefunctions of Fe^{2+} being the eigenstates of spin-Hamiltonian $\mathscr{H}_{\mathrm{Fe}}$ Eq. (4c). They can be written as superpositions of spin states $|S_3, m_3\rangle$ of Fe-ion with fixed z-projection m_3 of $\mathbf{S}_3$:

$$\Psi^{1}_{\mathrm{Fe}} = \frac{1}{\sqrt{2}}\left(|2,+1\rangle + |2,-1\rangle\right) \ , \qquad E_1 = D - 3E \ ,$$

$$\Psi^{2}_{\mathrm{Fe}} = \frac{1}{\sqrt{2}}\left(|2,+1\rangle - |2,-1\rangle\right) \ , \qquad E_2 = D + 3E \ ,$$

$$\Psi^{3}_{\mathrm{Fe}} = \frac{1}{\sqrt{2}}\left(|2,+2\rangle - |2,-2\rangle\right) \ , \qquad E_3 = 4D \ ,$$

$$\Psi^{4}_{\mathrm{Fe}} = \frac{a}{\sqrt{2}}\left(|2,+2\rangle - |2,-2\rangle\right) - b|2,0\rangle \ , \qquad E_4 = 2D\left(1 + \sqrt{1 + 3E^2/D^2}\right) \ ,$$

$$\Psi^{5}_{\mathrm{Fe}} = \frac{b}{\sqrt{2}}\left(|2,+2\rangle - |2,-2\rangle\right) + a|2,0\rangle \ , \qquad E_5 = 2D\left(1 - \sqrt{1 + 3E^2/D^2}\right) \ ,$$

where $a = \left(\sqrt{1 + 12E^2/E_4^2}\right)^{-1}$, $b = \left(\sqrt{1 + E_4^2/12E^2}\right)^{-1}$. The spin states Ψ^{j}_{Q} of a quinone pair are of definite parity:

$$\Psi^{1}_{\mathrm{Q}} = |S\rangle \ , \qquad \Psi^{2}_{\mathrm{Q}} = |T_0\rangle \ , \qquad \Psi^{3,4}_{\mathrm{Q}} = \left(|T_+\rangle \pm |T_-\rangle\right)/\sqrt{2} \ .$$

The set of the spin states Eq. (5) can be separated into four independent subsets not mixed by the interactions Eq. (4). This separation can be done due to following reasons. First, $\mathscr{H}$ is invariant under inversion of spins of all particles. It allows one to divide basis set Eq. (5) into subsets with even and odd spin states. Further, each of these subsets can be divided once more if we take into account that spin states Eq. (5) may be rewritten as superpositions of spin states $|S, M\rangle$ with even or odd z-projections M of the total spin of complex. Hamiltonian Eq. (4a) induces spin transitions only between the states with the same parity of M, since it can be rewritten as a bilinear form including terms of $(S_i^+)^2$, $(S_i^-)^2$, $S_3^+S_3^-$, $S_3^-S_3^+$ and S_{iz}^2 type only ($i = 1, 2, 3$). As a result, there are four different spin subsystems each involving five spin states:

(subset 1): $|1\rangle = \Psi^1_{Fe}\Psi^1_Q$, $|2\rangle = \Psi^2_{Fe}\Psi^2_Q$, $|3\rangle = \Psi^3_{Fe}\Psi^3_Q$, $|4\rangle = \Psi^4_{Fe}\Psi^4_Q$, $|5\rangle = \Psi^5_{Fe}\Psi^5_Q$.

(subset 2): $|1\rangle = \Psi^2_{Fe}\Psi^1_Q$, $|2\rangle = \Psi^1_{Fe}\Psi^2_Q$, $|3\rangle = \Psi^3_{Fe}\Psi^4_Q$, $|4\rangle = \Psi^4_{Fe}\Psi^3_Q$, $|5\rangle = \Psi^5_{Fe}\Psi^3_Q$.

(subset 3): $|1\rangle = \Psi^3_{Fe}\Psi^1_Q$, $|2\rangle = \Psi^1_{Fe}\Psi^3_Q$, $|3\rangle = \Psi^2_{Fe}\Psi^4_Q$, $|4\rangle = \Psi^4_{Fe}\Psi^2_Q$, $|5\rangle = \Psi^5_{Fe}\Psi^1_Q$.

(subset 4): $|1\rangle = \Psi^4_{Fe}\Psi^1_Q$, $|2\rangle = \Psi^5_{Fe}\Psi^1_Q$, $|3\rangle = \Psi^1_{Fe}\Psi^4_Q$, $|4\rangle = \Psi^2_{Fe}\Psi^3_Q$, $|5\rangle = \Psi^3_{Fe}\Psi^2_Q$.

This separation simplifies analysis, because the Hamiltonian matrix can be block diagonalized and the spin subsystems can be considered independently reducing the size of calculations. For the better visualization of spin dynamics we rewrite the matrices of the $\mathscr{H}' = \mathscr{H} - ik_S P_S/2$ for each of the subsets:

$$H'_1 = \begin{pmatrix} E_1 - 2J_0 - ik_S/2 & -\Delta J & -\Delta J & \Delta J_1 & \Delta J_4 \\ -\Delta J & E_2 & J_S & -J_{S2} & -J_{S3} \\ -\Delta J & J_S & E_3 & 2J_{Sa} & 2J_{Sb} \\ \Delta J_1 & -J_{S2} & 2J_{Sa} & E_4 & 0 \\ \Delta J_4 & -J_{S3} & 2J_{Sb} & 0 & E_5 \end{pmatrix}, \tag{6a}$$

$$H'_2 = \begin{pmatrix} E_2 - 2J_0 - ik_S/2 & -\Delta J & -\Delta J & \Delta J_2 & \Delta J_3 \\ -\Delta J & E_1 & -J_S & J_{S1} & J_{S4} \\ \Delta J & -J_S & E_3 & 2J_{Sa} & 2J_{Sb} \\ -\Delta J_2 & J_{S1} & 2J_{Sa} & E_4 & 0 \\ -\Delta J_3 & J_{S4} & 2J_{Sb} & 0 & E_5 \end{pmatrix}, \tag{6b}$$

$$H'_3 = \begin{pmatrix} E_3 - 2J_0 - ik_S/2 & \Delta J & \Delta J & -2a\Delta J & -2b\Delta J \\ \Delta J & E_1 & J_S & -J_{S1} & -J_{S2} \\ \Delta J & J_S & E_2 & J_{S2} & J_{S3} \\ -2a\Delta J & -J_{S1} & J_{S2} & E_4 & 0 \\ -2b\Delta J & -J_{S2} & J_{S3} & 0 & E_5 \end{pmatrix}, \tag{6c}$$

$$H'_4 = \begin{pmatrix} E_4 - 2J_0 - ik_S/2 & 0 & \Delta J_1 & \Delta J_2 & -2a\Delta J \\ 0 & E_5 - 2J_0 - ik_S/2 & \Delta J_4 & \Delta J_3 & -2b\Delta J \\ \Delta J_1 & \Delta J_4 & E_1 & J_S & J_S \\ \Delta J_2 & \Delta J_5 & J_S & E_2 & J_S \\ -2a\Delta J & -2b\Delta J & J_S & J_S & E_3 \end{pmatrix}, \tag{6d}$$

where the following designations are used:

$$\Delta J_1 = (a - \sqrt{3}b)\Delta J \quad , \qquad \Delta J_2 = (a + \sqrt{3}b)\Delta J \quad ,$$

$$\Delta J_3 = (a - \sqrt{3}a)\Delta J \ , \qquad \Delta J_4 = (b + \sqrt{3}a)\Delta J \ ,$$

$$J_S = J_1 + J_2 \ , \qquad J_{S1} = (a - \sqrt{3}b)J_S \ , \qquad J_{S2} = (a + \sqrt{3}b)J_S \ ,$$

$$J_{S3} = (b - \sqrt{3}a)J_S \ , \qquad J_{S4} = (b + \sqrt{3}a)J_S \ .$$

Equations of motion for the density matrix ρ_{ij}^{α} in a α-th subsystem ($\alpha = 1, ..., 4$) can be rewritten as

$$\frac{\partial \rho_{ij}^{\alpha}}{\partial t} = -\mathrm{i}[\mathscr{H}^{\alpha}, \rho^{\alpha}] - \frac{k_S}{2}(P_S\rho^{\alpha} + \rho^{\alpha}P_S)_{ij} - k\rho_{ij}^{\alpha} \ . \tag{7}$$

In this paper the model Eqs. (3), (4) is studied numerically. Initial populations of all spin states of the complex are suggested to be equal. In calculations we use the known values of ZFS parameters of Fe^{2+} in RC of *Rhodobacter sphaeroides* [18]: $D = 5.28$ cm^{-1}, $E = 1.33$ cm^{-1}. Rate constants $k_S = 10^4$ s^{-1} and $k = 10$ s^{-1} are taken from [10]. Values J_0, $\Delta J = |J_1 - J_2|$ and $J_S = |J_1 + J_2|$ are varied between -2 and 2 cm^{-1}, 0 and 0.5 cm^{-1}, -1 and 1 cm^{-1} [19, 20], respectively.

3 Numerical Method

In the Liouville space the equations of motion Eq. (7) for the density matrix ρ can be rewritten as a system of ordinary differential equations for the real vector $\sigma(t)$ [24]

$$\frac{\mathrm{d}\sigma_n(t)}{\mathrm{d}t} = \sum_{m=1}^{M} A_{nm}\sigma_m(t) \ , \qquad (n = 1, ..., M) \ . \tag{8}$$

Here the single index n runs through all possible combinations of index pair i, j and varies in $1, ..., M = N \times N$ range (N is a number of spin states). The components σ_n are defined as ρ_{ii} if $i = j$, $\mathrm{Re}\rho_{ij}$ if $i > j$, and $\mathrm{Im}\rho_{ij}$ if $i < j$; A_{nm} are the elements of corresponding matrix of $M \times M$ dimension.

The solution of Eq. (8) can be expressed in terms of eigenvectors B_m and eigenvalues λ_m of matrix A_{nm}

$$\sigma_n(t) = \sum_{m=1}^{M} C_m B_m^{(n)} \exp(\lambda_m t) \ , \qquad (n = 1, ..., M) \ , \tag{9}$$

where C_m are the coefficients of decomposition.

From Eq. (9) the reaction yield

$$Y = k_S \mathrm{Tr}\left(\mathbf{P}_S \int_0^{\infty} \rho(t)\,\mathrm{d}t \right) \ ,$$

is calculated as

$$Y = k_S \sum_{n=1}^{M} (P_S)_n \sum_{m=1}^{M} B_m^{(n)} \frac{C_m}{\lambda_m} \quad . \tag{10}$$

CIDEP of the Fe^{2+} ion is described in terms of the populations N_i of spin states Ψ_{Fe}^i. Deviation of the population of the i-th spin state from the initial population is calculated

$$\Delta N_i = \mathrm{Tr}(k_S \mathbf{P}_i^{Fe} \mathbf{R} + k \mathbf{P}_i^{Fe} \mathbf{R}) \ ,$$

where $\mathbf{R} = \int_0^\infty \boldsymbol{\rho}(t)\, dt$, $\mathbf{P}_i^{Fe} = |\Psi_{Fe}^i\rangle\langle\Psi_{Fe}^i|$ is the projection operator on the state Ψ_{Fe}^i.

Using Eq. (9) one obtains simple expressions for the ΔN_i

$$\Delta N_i = \sum_{n=1}^{M} \left(k_S (P_i^{Fe} P_S)_n + k (P_i^{Fe})_n\right) \sum_{m=1}^{M} B_m^{(n)} \frac{C_m}{\lambda_m} \ , \tag{11}$$

where $(P_S)_n$ is a matrix element of $\mathbf{P}_S$ in the basis set Eq. (5).

The problem of eigenvectors and eigenvalues was solved numerically [25]. Separation of Hamiltonian matrix into independent blocks allows us to reduce the size of computations since instead of 400×400 matrix one then must diagonalize four 25×25 matrices.

4 Results and Discussion

A scheme of transitions in quinone pair accounting for both the ET and singlet-triplet conversion can be pictured as

$$\begin{array}{ccccc} P \ldots Q_A Q_B^- & \xleftarrow[k]{\text{III}} & {}^1(Q_A^- Q_B^-) & \xrightarrow[k_S]{\text{I}} & {}^1(Q_A Q_B^{2-}) \\ & & \text{II} \updownarrow \Delta J & & \\ P \ldots Q_A Q_B^- & \xleftarrow[k]{\text{III}} & {}^3(Q_A^- Q_B^-) & & \end{array} \tag{12}$$

where ${}^1(Q_A^- Q_B^-)$ and ${}^3(Q_A^- Q_B^-)$ are the reactant subensembles in singlet and triplet states, respectively; ${}^1(Q_A Q_B^{2-})$ is the product of the reaction. Process I represents the electron transfer in singlet pairs with the rate constant k_S; II – spin conversion in reactants; III – back electron transfer from Q_A^- to the primary electron donor P^+ with the rate constant k.

4.1 Effect of ZFS on the Efficiency of the ET

An analysis of the expressions for the spin Hamiltonian matrices H_{ij}^{α} Eqs. (6) gives an insight into some general features of spin dynamics of the complex.

First of all, it is seen that ST-transitions in $Q_A^- Q_B^-$ pair are induced only in the case of asymmetric spin exchange interaction between Fe^{2+} and quinones, when $\Delta J = |J_1 - J_2| \neq 0$. This result is well-known in the theory of spin catalysis (see, e.g., [3, 5]). Larger values $|\Delta J|$ ($\Delta J > J_0$) facilitate spin conversion and promote more effective indirect ET from triplet pairs (consequent stages II and I in the scheme Eq. (12)). However, it is known [5] that the isotropic exchange interactions Eq. (4b) in a three-spin system are able to induce multiplet transformation only for 1/3 part of all triplet states. Because of the conservation of the total spin of the complex $\mathbf{S} = \mathbf{S}_1 + \mathbf{S}_2 + \mathbf{S}_3$ the states with $S = S_3 + 1$ and $S = S_2 - 1$ are not involved into ST-conversion.

Situation becomes somewhat different in the presence of anisotropic interactions between the particles. In this case S or/and S_z are no longer conserved and some additional spin states with triplet quinone pair enter into ST-conversion. The ZFS interactions Eq. (4c) provide one of the possible ways to enhance the efficiency of spin catalysis. Numerical analysis shows that the ZFS can potentially raise the reaction yield in a three-spin system up to 100%.

However, in the case of very large ZFS (D, $E \gg J_i$) one should expect a decrease of the reaction yield with the increase of D and E because the ZFS then bring the main contribution in energy splittings between the spin states (it is easily seen from the Hamiltonian matrices Eq. (6)). In bacterial RCs the ZFS parameters D and E exceed possible values $|\Delta J|$ since the absolute values of J_1 and J_2 are known to be in the 0.06–0.4 cm^{-1} range [19, 20]. $|\Delta J_0|$ is also estimated to be less then 1 cm^{-1}. In this context the ST-conversion of the majority of triplet spin states is suppressed and the singlet product yield cannot be very high.

This conclusion is verified by numerical calculations presented below. Figure 1 represents the plots of the reaction yield Y versus J_0 for the different ΔJ. All calculated values of Y lie in the 0.5–0.8 range. The reaction yield exhibits very

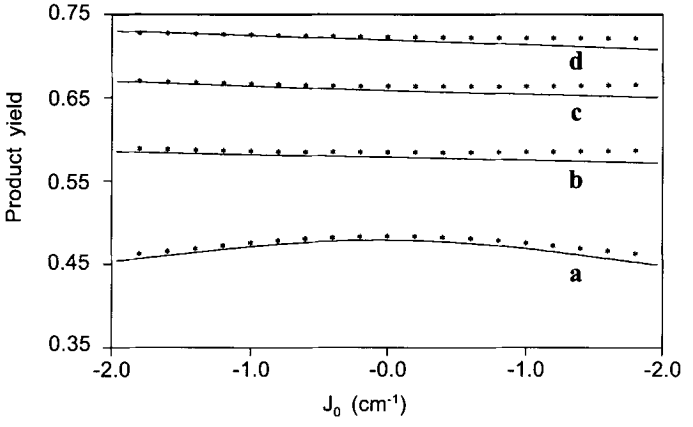

Fig. 1. Singlet yield of the ET reaction as a function of J_0 for the different ΔJ. Solid curves – numerical results, asterisks – kinetic approximation Eq. (16). The parameters used: $J_S = 0$, $\Delta J = 0.1$ (**a**), 0.2 (**b**), 0.3 (**c**), 0.4 (**d**) cm^{-1}. The values D, E, k_S and k are given in text.

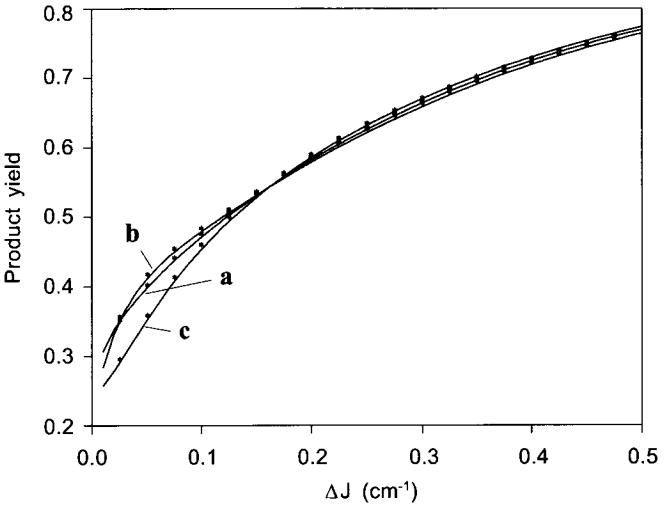

Fig. 2. Reaction yield as a function of ΔJ for different J_0. Solid curves – numerical results, asterisks – calculated from Eq. (16). The parameters used: $J_S = 0$, $J_0 = 1$ (**a**), 0 (**b**), -1 (**c**) cm^{-1}.

weak dependence on the parameters J_0 and J_S, and strong dependence on ΔJ. $Y(\Delta J)$ plots are pictured in Fig. 2.

4.2 Kinetic Approximation

In the case of large ZFS (D, $E \gg J_i$) we can introduce considerable simplifications in the model Eqs. (2)–(4) and obtain analytical expressions for spin and reaction dynamics. Due to large ZFS the ST-splittings between spin states in subsystems G_k greatly exceed the corresponding off-diagonal elements H_{ij} responsible for ST-transitions. In this situation the rates of indirect ET in triplet pairs are significantly less than the ET rates in singlet pairs. It can be shown that the population dynamics $n_i(t)$ of all spin states $\Psi^{(i)}$ of reactants is then well-fitted by a single exponential function

$$n_i \sim \exp(-k_i t) \ .$$

The problem thus reduces to obtaining k_i determining the rates of ET reaction in an individual spin states. The validity of the approach was discussed in [23].

Due to weak dependence of the reaction yield Y on J_0 and J_S we can set them to zero ($J_S = J_0 = 0$). Spin dynamics of the subsystems G_k with a good accuracy can be separated into dynamics of the individual pairs of states each consisting of fast-decaying singlet state and slowly decaying triplet one. The population dynamics of such a coupled singlet-triplet diad are studied analytically and for the case of weak ST-coupling ($\alpha \ll 1$) one obtains

$$n^S(t) \simeq (1/2)\exp(-k^1 t) \ , \qquad k^1 = k^S \ , \tag{13}$$

$$n^{T}(t) \simeq (1/2)\exp(-k^2 t) \ , \qquad k^2 = \alpha k^{S} \ , \tag{14}$$

where $\alpha = \omega^2/(\Delta E^2 + k_S^2)$; $n^S(t)$, $n^T(t)$ are populations of S- and T-states of a diad; ΔE and ω are the energy splitting in the diad and the corresponding off-diagonal matrix element of ST-mixing.

For the spin dynamics of reactants one obtains:

$$P(t) \simeq \frac{1}{20}\left(5\exp(-k_S t) + \sum_{i=1}^{15}\exp(-k_i^T t)\right) \ ,$$

$$k_i^T = \alpha_i k_S \ , \qquad \alpha_i = \frac{\omega_i^2}{\Delta E_i^2 + k_S^2} \ . \tag{15}$$

Here the parameters ω_i are equal to the corresponding off-diagonal matrix element of H_α Eqs. (6). With Eq. (15) the singlet reaction yield is calculated as

$$Y = \frac{1}{4}\frac{k}{k + k_S} + \frac{1}{20}\sum_{i=1}^{15}\frac{k}{k + k_i^T} \ . \tag{16}$$

Equation (16) gives a good analytical approximation for all numerical data obtained. The difference between the numerical results and the estimation Eq. (16) does not exceed 3–5% in the whole range of parameters J_i. The values of Y, calculated according to Eq. (16), are presented in Figs. 1 and 2 by the asterisks.

The expression Eqs. (13)–(15) can be used for an estimation of an efficiency of charge transfer between quinones in bacterial reaction centres. Taking $k_S \sim 10^4$

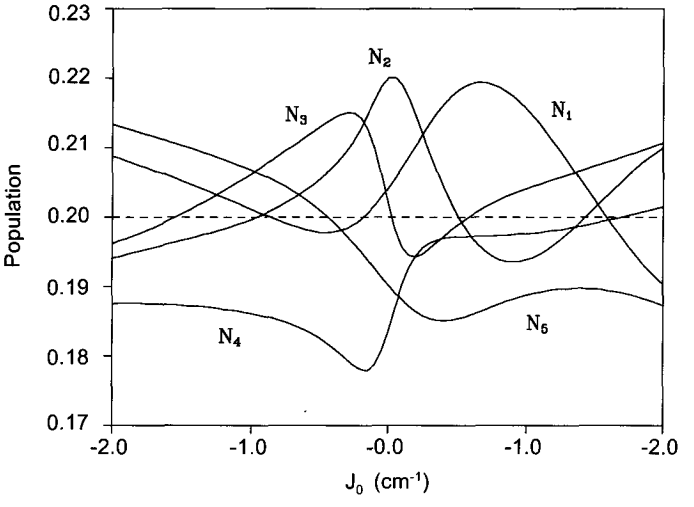

Fig. 3. The dependence of populations of spin states of Fe $N_i = N(\Psi_{Fe}^i)$, $i = 1, ..., 5$ on the parameter of exchange interactions $J_S = J_1 + J_2$. Here the following of parameters are used: $\Delta J = 0.3$ cm^{-1}, $J_0 = 0$.

s^{-1}, $\Delta J \sim 0.25$ cm^{-1} and $J_0 = 0$, we obtain that ten spin states of the complex decay with the rate constant approximately equal to (or less than) $k_{min} \sim k_S \cdot 10^{-4}$ and the remaining spin states decay still faster than k_{min}. In this case the efficiency of back ET ($k \sim 10$ s^{-1} [6, 7]) is equal to $k/2(k + k_{min}) \sim 0.5$. The efficiency of direct ET is then estimated to be ~50%. Note that due to strong ΔJ-dependence the reaction yield can be much higher for another parameter set. For example, if $\Delta J \sim 2$ cm^{-1}, the reaction yield increases to ~80% (only four spin states of complex decay slower than k_{min}).

It should be pointed out that spin-selective ET between quinone anion-radicals generates electron spin polarization in the complex. This polarization is associated with the formation of nonequilibrium populations of spin states of Fe^{2+}. We suppose that the initial weights of any spin states in the three-spin system are equal at the initial moment. Due to ET reaction in singlet anion-radical pairs and spin conversion the difference in the populations of the eigenstates of H_{Fe} Eq. (4c) arises. The populations $N_i = N(\Psi_i^{(Fe)})$, $i = 1, ..., 5$ as functions of J_S are plotted in Fig. 3.

5 Conclusions

In conclusion we briefly summarize the results of the present study. To clarify the spin-catalytic influence of Fe^{2+} on the ET reaction between Q_A^- and Q_B^- in reaction center of photosynthetic bacteria a theoretical model accounting for spin and reaction dynamics in $Q_A^-Fe^{2+}Q_B^-$-complex is proposed and investigated. It is shown that exchange interactions of Fe^{2+} with quinone anion-radicals are capable to produce fast singlet-triplet conversion in $Q_A^-Q_B^-$-pairs with rates higher than the rate of back electron recombination with primary donor P^+. Spin conversion exerts considerable influence on the reaction dynamics, and under certain conditions the reaction yield can be altered over tens of per cent. The rate of singlet-triplet transitions is shown to depend strongly on the parameter of asymmetry of $Fe^{2+}Q_i^-$ spin exchange ($\Delta J = J_1 - J_2$), so the opposite signs of J_1 and J_2 are expected to favour both the ST-mixing and reaction yield enhancement.

Acknowledgements

The work was supported by INTAS (grant 96-1275) and Russian Foundation for Basic Research (grant 98-03-33136a). We are grateful to Kev Salikhov and Anatoli Shushin for helpful discussions.

References

1. Salikhov K.M., Molin Yu.N., Sagdeev R.Z., Buchachenko A.L.: Spin Polarization and Magnetic Effects in Radical Reactions. Budapest: Akademian Kiado & Amsterdam: Elsevier 1984.
2. Step E.N., Buchachenko A.L., Turro N.J.: J. Am. Chem. Soc. **116**, 5446 (1994)

3. Buchachenko A.L., Step E.N., Ruban V.L., Turro N.J.: Chem. Phys. Lett. **223**, 315 (1995)
4. Hoff A.J., Hore P.J.: Chem. Phys. Lett. **108**, 104–110 (1984)
5. Buchachenko A.L., Berdinsky V.L.: Izv. Akad. Nauk, Ser. Khim. 1646–1652 (1995)
6. Okamura M.Y., Feher G., Nelson N. in: Photosynthesis: Energy Conversion by Plants and Bacteria (Govindjee, ed.), vol. 1, p. 195. New York: Academic Press 1982.
7. Parson W.W., Ke B. in: Photosynthesis: Energy Conversion by Plants and Bacteria (Govindjee, ed.), vol. 1, p. 331. New York: Academic Press 1982.
8. Feher G., Okamura M.Y.: Brookhaven Symp. Biol. **28**, 183–194 (1979)
9. Leigh J.S., Dutton P.L.: Ann. N.Y. Acad. Sci. 883–845 (1973)
10. Parson W.W.: Biochim. Biophys. Acta **189**, 384–396 (1969)
11. Debrunner P.G., Schultz C.E., Feher G., Okamura M.Y.: Biophys. Soc. Abstr. **15**, 226a (1975)
12. Boso B., Debrunner P.G., Okamura M.Y., Feher G.: Biochim. Biophys. Acta **638**, 173–177 (1981)
13. Okamura M.Y., Isaacson M.I., Feher G.: Proc. Natl. Acad. Sci. USA **72**, 3491 (1975)
14. Dutton P.L., Prince R.C., Tiede D.M.: Photochem. Photobiol. **28**, 939–949 (1978)
15. Wraight C.A.: Photochem. Photobiol. **30**, 767–776 (1979)
16. Kirmaier C., Holten D., Debus R.J., Feher G., Okamura M.Y.: Proc. Natl. Acad. Sci. USA **83**, 6407–6411 (1986)
17. Weiner P., Kollman P.: J. Comp. Chem. **2**, 283–303 (1981)
18. Butler W.F., Johnston D.C., Shore H.B., Fredkin D.R., Okamura M.Y., Feher G.: Biophys. J. **32**, 967 (1980)
19. Butler W.F., Calvo R., Fredkin D.R., Isaacson M.I., Okamura M.Y., Feher G.: Biophys. J. **45**, 947–973 (1984)
20. Dismukes G.C., Frank H.A., Friesner R., Sauer K.: Biochim. Biophys. Acta **764**, 253–271 (1984)
21. Pedersen J.B., Freed J.H.: J. Chem. Phys. **58**, 2746 (1973)
22. Pedersen J.B., Freed J.H.: J. Chem. Phys. **59**, 2869 (1973)
23. Pedersen J.B., Shushin A.I., Jorgensen J.S.: Chem. Phys. **189**, 479 (1994)
24. Mukamel S.: Principles of Nonlinear Optical Spectroscopy. Oxford: Oxford University Press 1995.
25. Press W.H., Flannery B.P., Teukolsky S.A.: Numerical Recipes. New York: Cambridge University 1986.

Authors' address: Dr. Anatolii I. Ivanov, Department of Physics, Volgograd State University, Prodolnaya str. 30, 400062 Volgograd, Russian Federation